An Assessment of Fluid Inclusions Composition Using the Raman Spectroscopy at Daleishan Goldfield, Dawu County, Hubei Province, P.R. China.

Diarra Karim [1*], Hanlie Hong [2]

[1]China University of Geosciences, Wuhan, 430074, China
[2] Faculty of Earth Sciences, China University of Geosciences, Wuhan, 430074 (Hubei province), China
[*]Corresponding Author: E mail: bn_cogem@yahoo.fr

Abstract: The purpose was to assess fluid inclusions composition in the Goldfield, Hubei province, China. The laser Raman spectroscopy was used as an analytical tool. The results show that water and carbon dioxide (70 %), and quartz (10 %) are the primary and secondary compositions of most of the inclusions, respectively. A number of three phase inclusions were low and inclusion size varies from 1 to 27µm. The density of CO2 fluid inclusions measured in quartz mineral varied from 0.61 to 0.96 g/cm3. No traces of other gases such as hydrogen (H2), ethylene (C2H2), ethene (C2H4), benzene (C6H6), hydrogen sulphide (H2S) and carbon monoxide (CO) were observed, confirming epithermal origin of the deposit (quartz ± calcite± adularia ± illite assemblage). In Daleishan goldfield, according to inclusion composition, vapor and liquid may be main agent transports for gold in epithermal systems as well as for silver. [Journal of American Science 2010;6(7):30-37]. (ISSN: 1545-1003).

Key words: Auriferous veins, Raman spectroscopy, inclusions fluids, Daleishan Goldfield, quartz.

1. INTRODUCTION

Interest in study of fluid inclusions in the Earth Sciences goes back to works of the founding father of fluid inclusions, Sorby (1858) whom described samples from ore deposits containing fluid inclusions and drew conclusions concerning ore formation. The modern science of fluids inclusion geochemistry grew principally out of pioneering work on hydrothermal ore deposits more than 50 years ago (Roedder, 1958). The plethora of researches on fluid inclusions composition in mineral deposits is a testimony to this concern (K.A.A. Hein et al. (2006) have linked mineral and fluid inclusion paragenetic studies at The Batman deposit, Mt. Todd (Yimuyn Manjerr) goldfield, Australia; Yunshuen Wang et al. (1999) proved that fluid inclusion data indicate that the hydrothermal fluids are related to ore deposition of the high sulfidation Au–Cu deposits at Chinkuashih, Taiwan; Campbell and Panter (1990) showed, using infra-red microscopy, that inclusions in quartz intergrown with cassiterite and wolframite had different microthermometric properties to those hosted by the ore minerals themselves; Roedder, 1984; Van den Kerkhof et al. (2001) provided standard criteria for the recognition of primary, pseudo-secondary and secondary inclusions.

However, poorly developed spectroscopic methods and microthermometry often characterized most of the methods used in field investigations. During the last 20 years, analytical techniques to include the laser Raman spectroscopy (*MOLE, (1976) and LABRAM or the system 1000/2000/3000 Renishaw (1997) are the first and the newest Raman microspectrometers)* have improved significantly as has the quality of data obtained (Roedder, 1984; Pasteris *et al.*, 1987; Li Binglun et al., 1986; Lu Huang Zhang et al., 1990; Rosso et al., 1995; 1997; Yamamoto et al., 2006; 2007).

In geology, Raman spectroscopy is used for testing of materials, and especially for analysis of materials in inclusions; Raman spectroscopy provides an efficient, non-destructive and sensitive tool allowing for an assessment of fluid inclusions composition and estimation of the pressures (Wopenka *et al.*, 1990; Burke A.J. E., 2001, Rosso et al., 1995; Yamamoto et al., 2006; 2007).

Studies on fluid inclusions composition in mineral deposits, especially gold deposits in China have a long history (Roedder, E., 1967, 1977a, 1979; Anderson et al., 1981, 1995; M.R., Bodnar et al., 1985 T.J., Kuehn, et al., 1989, 1991, 1994; Groves, D.I. *et al.* 1992; Heinrich, C.A et al., 1992; Sheng Jify et al., 1995; Xiao Long, et al. 2005; Roedder, E., et al. 1997; Audetat, A., et al., 1985; 1998; Hedenquist, J.W., et al., 1998*)*. In Daleishan goldfield Dawu County, many researches have been carried out since 1973. However, such studies focused on characteristics (dimension, morphology, etc) of quartz veins, texture and structure of ore minerals, genesis and model of deposit, geochemistry characteristics of lamprophyre and ore, etc. (Geological Party of Ordos Basin Northeast, Hubei Province, 1973-2009; Li Jiangzhou *et al.* 1990; Hong Hanlie *et al.* 1997; 2008; 2009 Zhou Hanwen *et al.*, 1998; Du Dengwen *et al.* 2008; 2009). Studies on compositions of fluid inclusion, are still in their juvenile and taking into consideration the fact that climate change may upset natural processes in the crust, there is need for up to date information, to serve as guide in exploration and mining planning and improved interpretation of gold ore formation. It is within this context that this study was conducted.

The purpose of this study was therefore assessing fluid inclusions composition at Daleishan Goldfield, Dawu County, Hubei Province, China, using Raman Spectroscopy. A better understanding of information on inclusion composition, through quartz mineral, over time should elucidate effective modeling and hence, the trapping of conditions of fluid inclusions and gold transport conditions in the region and beyond.

2. MATERIALS AND METHODS

2. Materials and Methods

2.1 Study Area

The study area *or Daleishan* Goldfield (longitude *114°08'37"N and latitude 31°29'08" S)* is located in Dawu County, Hubei Province, in central China. Daleishan goldfield including two (2) gold deposits namely, Baiyun and Dapoding, is also located in Daleishan dome center, which uplifts between Dabieshan and Tongbai Mountains. Dapoding gold district is at present the biggest gold deposit discovered in northeast Ordos *Basin (5.14 and 56.76 t of gold and silver, respectively, Hong Hanlie et al. 2009) whereas Baiyun gold deposit has mined out.* Both deposits belong to (3) three ore zones of Hubei province: the Tongbai-Dabieshan Mountains polymetallic zone, the Dawu-Hong'an copper-silver zone, and the Daleishan Mountain goldfield. (Fig. 1).

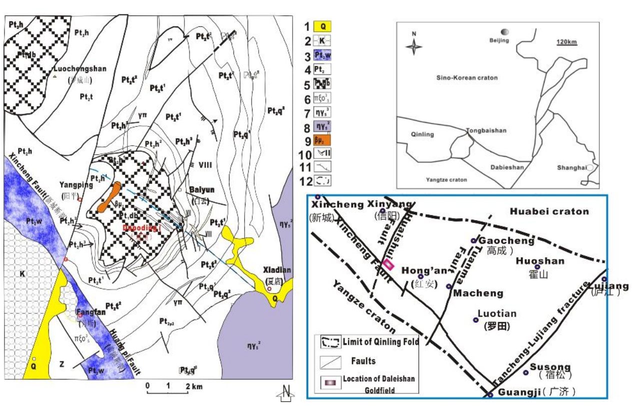

Fig 1. Simplified Geological Map of Daleishan Goldfield, modified after Du et al., 2009

The prospect temperate climate belongs to continental subtropical season; sun is shining adequately; rainfall is abundant and frost period is short; humidity rate and mean temperature are 0.93 and 15.9^{0} C, respectively. Also, highest and lowest temperatures observed in June and January are 40 and -16.5°, respectively. Although rainy season is relatively short, from mid-June to mid-July, annual mean rainfall is 328.0mm; north and south are wind directions during winter and summer respectively. Deposit district is constituted by a range of low-to high mountains, following WNW and ENE directions; peak and lowest altitudes, above sea level, are 626.2 and 65.80 m, respectively.

Main rocks distributed, in the district, are (1) Lower Proterozoic metamorphic complex rocks of Dabieshan Mountain, and (2) Middle Proterozoic rocks of Hong'an. Lower Proterozoic metamorphic complex rocks of Dabieshan Mountain cover Daleishan dome center while surrounding rocks are consisted of rocks of Hong' an; the two groups of rocks show parallel structures in conformable contact. Lamprophyre and granite porphyry dikes, distributed along faults of different directions, are developed; rocks of different magmatic periods, namely granite of Yanshanian period that is related to gold (silver) mineralization, outcrop in the gold district.

At Daleishan goldfield, with 5.14 and 56.76 tons gold and silver, respectively, two ore types are dominant: gold-hosted-quartz vein and gold-hosted-altered rocks; gold grade is *4-11.63 g/t*. Vein ore mineral, according to statistics, consists of quartz (60%), k-feldspar (15%), sericite (15%), sulphide (8%) and other minerals (2%). Ore-forming phase include hydrothermal mineralization period and supergene ore-forming phase, respectively. Gold and silver are useful component of Dapoding gold deposit. Gold (silver) mineralization distribution is strictly controlled by Daleishan dome and faults of WNW and NNE directions. Even if lamprophyres have intimate relation with gold mineralization controlled by Dabie rocks, hydrothermal fluid, meteoric water and other fluids contributed significantly to formation of ore-forming mass.

2.2. Sampling Design

The samples studied here are from two gold deposits (1) Baiyun and (2) Dapoding that form Daleishan goldfield. Because gold mineralization is related to quartz veins, nine (9) hand picking samples, a least 1 kg weight, were collected, in July 2008, from three (3) of thirteen (13) auriferous veins of the goldfield, from core to rim. Two veins of Baiyun gold deposit district, No I and II, and one vein (No X) of Dapoding deposit were selected. On the whole, 5, 2 and 1 samples were collected from veins No I, II and X, respectively.

Double-polished (50-150μm) and ordinary standard thin sections of quartz were prepared at Sample Pre-treatment Bureau of China University of Geosciences, Wuhan, China. Five (5) double-polished sections (1--1;1-2-1; 1-3-1;2-1and 10-1-1) and 10 standard thin sections, four (4) from vein No I（1-2-1;1-3-1; 1-3-2; 1-4-1）, four (4) from vein No 2 (2-2-1;2-2-2; 2-2-3;2-2-4), and two (2) from vein No X (10-1-1;10-1-2), sections were prepared using epoxy and resins.

2.3. Data collection and Analyses

First, microscopic observations were done, on double-polished, thin sections on Linkam THM SG600 infra-red microscope in order to collect information such as type, morphology, size, liquid-vapor ratio, distribution, origin of inclusions. Simultaneous pictographs of inclusions were taken. Main host- mineral of inclusions were determined too. All data collected were reported in table (Table 1). Each thin section or polished section was carefully examined in paying attention to different types of inclusion present, namely (1) CO_2 inclusion (2) three phase inclusion, and (3) liquid vapor phase inclusion. Representatives of each type of inclusion were selected, described, and pictures were taken under polarized-light. Infra-red microscope Linkam THM SG600 Microscope could not make composition analysis of individual inclusions, so Raman spectroscopy, Renishaw RM-1000, was selected for that. Because of limitations imposed by the minimum of sampling volume of the Raman system, only inclusions with a diameter above 5μm were selected for Raman analysis. Therefore, composition analysis has been carried out on a total of seven (7) inclusions, from 3 thin sections (1-2-1, 2-2-1 and 10-1-2) were selected.
Secondly, thin sections selected for Raman analysis were cleaned using ethanol in order to avoid surface fluorescence which can be due to incompletely dissolved remnants of epoxy and resins used in the preparation of samples.

Analysis of single fluid inclusions and solid inclusions were do using the Raman spectroscopy Renishaw RM-1000 System equipped with a microscope stage, built at State Key Laboratory of Geological Processes and Mineral Resources, located at China University of Geosciences (Wuhan). Excitation was provided by 514.5nm line of Argon-ion laser at 3.4mW, focused to a spot size of 1.5μm. Spectra were measured with spectrometer entrance slits at 12.5μm. Scanning power efficiency of fluid inclusion composition and solid inclusions are 10W, 5-20nW, respectively; counting time is 20s. First scanning is carried out from 0 to 4000 cm -1, and then second and third scanning are carried out according to peak reduced resolution zone. Data consisted of wavelength (cm^{-1}) and Raman counts that can be processed with softwares such as Excel 2007, Origin 8.0, and SPSS 17.0 for building spectrum. Raman signal from fluid-inclusion were recorded on computer screen (Fig.4), the background subtracted using Lorenz Method. For the qualitative analysis of Raman active species (identification) in fluid inclusions, only the Δv values of their characteristics are necessary species presence can be confirmed by their particular peaks in the spectrum.

3. RESULTS

3.1. Inclusion studies

Inclusion petrography, according to data collected from various inclusions under microscope, indicates that inclusions inside quartz grains are usually developed; 3 types of inclusions are notified according to their characteristics (1) CO_2 inclusion (2) three phase inclusion, and (3) liquid vapor phase inclusion., occupying large proportion, Liquid vapor two-phase is followed by single CO_2 phase, whereas a few numbers of three phase inclusion have been reported, particularly in inclusions from veins no I and II. Inclusions are, inside quartz mineral, usually are grouped, aligned or randomly distributed; their morphology is regular and present primary origin (Fig.2).

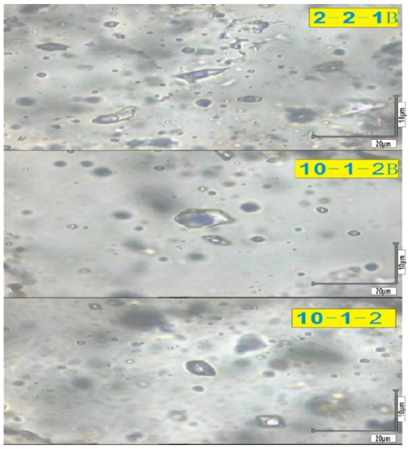

Figure.2. Photomicrographs of fluid inclusions in quartz, during Raman spectrometry analysis, from The Daleishan goldfield, Hubei Province, China.
Source : Authors' research

CO_2 inclusions present two (2) phases, with 40 to 70 % of total inclusion occupied by vapor; their sizes vary from 4 to 8μm and this type of inclusions present circular form.

Three phase inclusion usually present H_2O (l) + CO_2 (l) + CO_2 (g) (Fig.2D); its size varies from 7 to 25μm. Even though spherical, ellipsoidal, and lozenge shapes characterize most of three phase inclusion, a few numbers present regular forms. CO_2 volume, occupies at least 50% of total volume, numerous CO_2 volume up to 80% are also found.

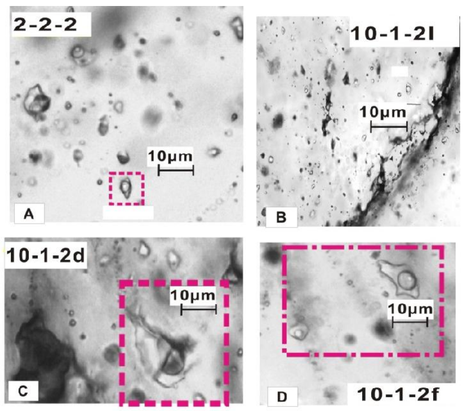

Fig.3. Examples of fluid inclusions in quartz from Daleishan goldfield. (A) sample2-2-2; isolated three phase primary inclusions with negative crystal faces; some are connected (right corner). (B) Sample 10-1-2l; CO_2 inclusion, liquid vapor, and three phases located along fractures; some inclusions are connected. (C), (D) and Samples 10-1-2d;10.-1-2f, large primary three phase inclusions with negative crystal faces, in the background- minute trails of planar inclusions for (D).All pictographs are from polarized light of Linkam THM-SG 600
Source : Authors' research

Consisting main inclusion in quartz mineral grain, liquid vapor inclusions regroup vapor bubble. Vapor liquid ratio varies between 40 and 60 % and can reach 80 %. Liquid vapor two phase inclusions present ellipsoidal, spherical and circular shapes whereas a few numbers, of the same type of inclusions present irregular shapes with size varying from 4 to 7μm.

Inclusions sizes of samples collected from veins no I and II are smaller than those of auriferous vein no X. Auriferous vein no X was mined, when samples were collected meanwhile veins no I and II were been mined out.

3.2. Inclusion composition by Raman spectroscopy analysis

Tests have been carried out on different types of inclusions (CO_2 vapor, vapor liquid and three phase inclusions) collected from different auriferous quartz veins of the deposit. Results indicated that water and dioxide carbon (CO_2) (Fig.2) are and main contents of all types of inclusions, namely three phase inclusions, liquid vapor two phase inclusion, liquid phase inclusion and vapor phase inclusion. The Raman spectra of water (broad bands of several hundred cm^{-1}) present two peaks at 3219 and at 3657 cm^{-1} , representing H_2O liquid and H_2O vapor, respectively (Dubessy *et al.*,1992; Chen *et al* 1990). Raman spectra showed no trace of other gases such as H_2, C_2H_2, C_2H_4, C_6H_6, H_2S and CO, etc as well as SO_4^{2-} and HCO_3 ions. Fluid inclusions studied here are almost all primary inclusions.

According to Raman spectroscopy analysis on inclusions, high content of water and dioxide (CO_2) is one characteristic of ore-fluid composition at Daleishan goldfield (Dapoding and Baiyun gold deposits). Obtained Raman spectra of CO_2 (v_1 : 1383 cm^{-1} and $2v_2$: 1279 cm^{-1}) have a downshift, from common Fermi diad of CO_2 (v_1 : 1388 cm^{-1} and $2v_2$: 1285 cm^{-1}), of 5 and 6 cm^{-1} ,respectively.

However, one inclusion, from sample 10-1-2A, in addition of CO_2 spectra, shows spectra of quartz inclusion at 464 and at 1160 cm^{-1}. The first spectrum of quartz, at 464 cm^{-1}, have only a downshift of 1cm^{-1} of the strongest peak of quartz, 466 cm^{-1} whereas the second spectrum of quartz (1160 cm^{-1}) represents one of the relatively strongest peaks of quartz (128, 206, 1082, and 1160 cm^{-1}). CO_2 spectra obtained with multi-channel from small inclusions (<20μm) in quartz always contain the Δv= 1160cm^{-1} peak of quartz.

Raman spectra, of seven (7) fluid inclusions, selected according to their types (CO_2 inclusions, three phase inclusion, and liquid vapor inclusions), provided water, CO_2 and quartz. Dominant Raman shift of dioxide carbon in relic inclusion assemblage of quartz ranged between 1383 cm^{-1} and 1279cm^{-1}, and 464 cm^{-1} in quartz （Fig.4）. A large proportion of inclusions, examined under Raman spectroscopy, contain water and CO_2 (70 %), and quartz (10 %) of total inclusions meanwhile a few inclusions, in addition to water and dioxide carbon (CO_2), are quartz. A total of 45 inclusions were examined under a microscope and data about size, type, morphology, liquid-vapor ratio, distribution and origin of inclusions, collected (Table 1). The sizes vary from 1 to 27μm (Fig. 5).

The Δv value of CO_2 was 104 cm^{-1} ($2v_2$-v_1; Yamamoto and Kagi, 2006; 2007)) making the densities of CO_2 fluid inclusion vary from 0.61 to 0.96 g/cm^3.

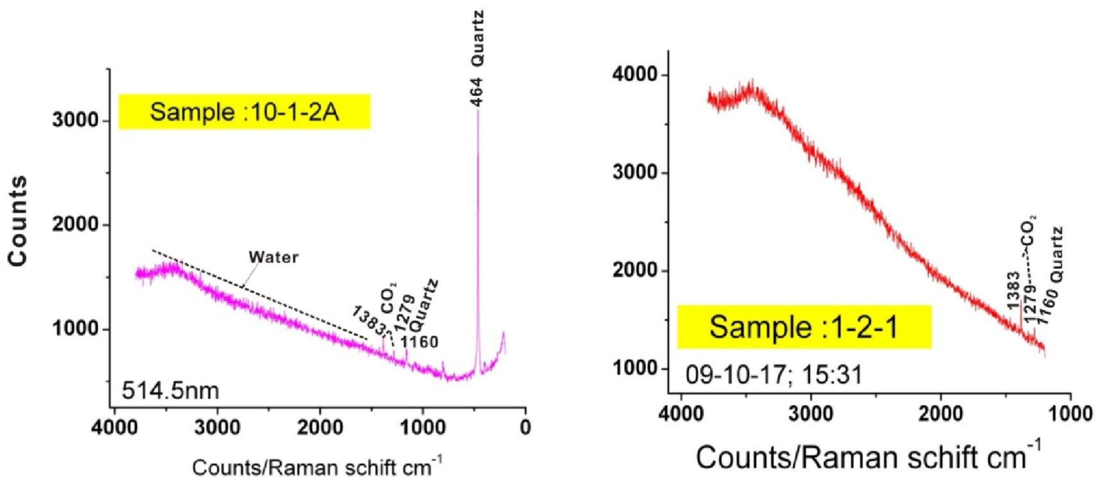

Fig.4 Raman spectrum of some inclusion
Source : Author's research

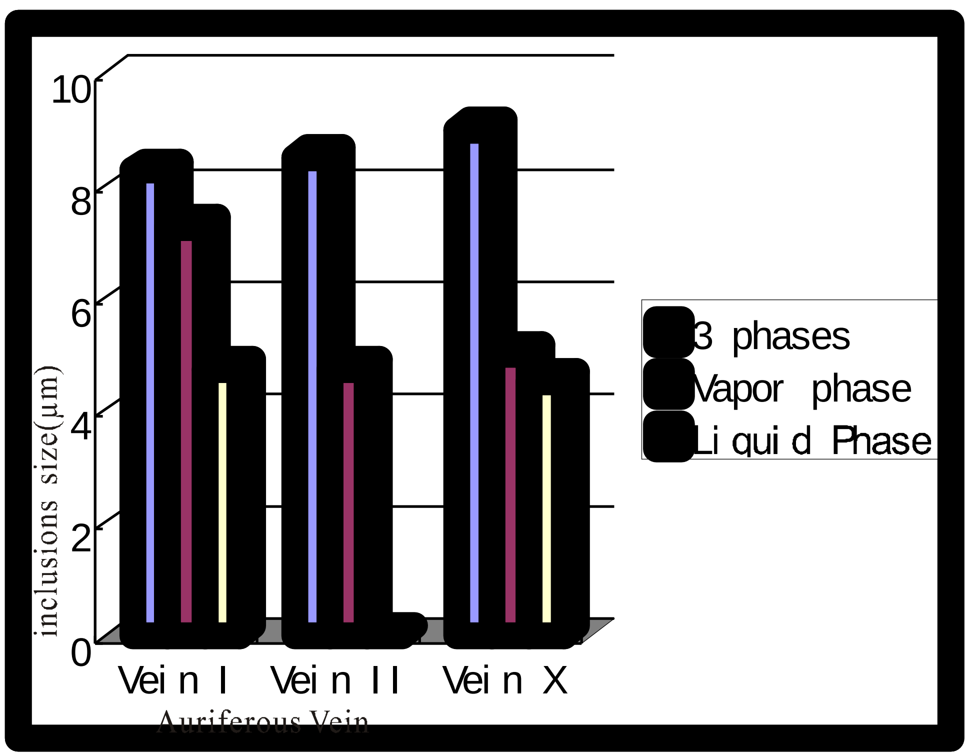

Fig.5 Mean size of different types of inclusions from different auriferous veins
Source : Authors' research

Table 1: Documentation Table of Inclusions

Vein no	Sample number	Phase type	Size (µm)	Vapor liquid ratio	distribution	Main minerals	Genesis	Photo no
X	FI-10-1-2	3 phases	5-7	3：2：5	group	quartz	primary	10-1-2k
II	FI-2-2-1	3 phases	6-8µm	3:1:6	group	quartz	primary	FI-2-2-1a
I	FI-1-2-1	Thunder vapor phase	4	6:4	Group	Idem	primary	1-2-1a
I	FI-1-2-1	Pure liquid phase	2	6 : 4	group	idem	primary	1-2-1b

Source: Author's research

4. Discussion

According to previous research achievements, Daleishan goldfield is an epithermal deposit that ore – forming depth is from 0.5 to 1.65 km below the water table (Geological Bureau in charge of Ordos Basin Northeast, Hubei Province, 1995). The deposit is principally linked to magmatism of Yanshanian period adamellite, where the magmatic input is entrained in and diluted by a structurally controlled or topographically driven large scale geothermal system. Epithermal deposits composed of this assemblage form in geothermal systems in volcanic arcs and rifts and result from the deep circulation of meteoric water, in Dabie Group rocks and Hong'an Group formations driven principally by a shallow intrusion. Deep down, the chloride-dominated waters are near neutral and contain reduced S-species adularia and platy calcites as deposits. During boiling of the ascending fluid, dissolved CO_2 and H_2S are partitioned into e vapor, which rises to the surface and condenses into the cool ground water, forming CO_2 –rich ground water, forming CO_2- rich or H_2S-rich steam-heated water. The CO_2 –rich or H_2S ground water is concentrated along the shallow margins of the up flow zones, where carbonate mineral-rich assemblage forms. In addition, because molecular interactions are stronger between CO_2 and H_2O for the system H_2O–CO_2- CH_4 (Dubessy *et al.*1999) may evaporate during magmatic process.

Co/Ni ratio of pyrite, superior to 1, suggests that gold mineralization is related to deep process. Only a limited number of species in fluid inclusions can be analyzed quantitatively, namely the polyatomic gas species and very few polyatomic gas species and polynuclear species in solution ($^{12}CO_2$, CH_4, N_2, H_2S, C_2H_2, SO_2, CO, NH_3, etc.) (Roedder, 1990). Therefore, further analyses such as LA-ICP–MS or PIXE, of inclusions, are needed for tracking other components like major and minor ions (Na, k, Ca, Mg, Cl, Mg, Li, Al, Fe, B, Ba, P) in liquid species or for quantitative analyses of solid species. Fluid inclusion composition provided by Raman spectroscopy suggests that dioxide carbon (CO_2), consisting main component, may play important role in gold (silver) mobilization and transport, from deep to the near-surface at Daleishan goldfield.

5. Conclusion

Raman spectra, of seven (7) fluid inclusions, present peaks of water, dioxide (CO_2) and quartz species. A large proportion of inclusions, examined under Raman spectroscopy, contain water and CO_2 (> 70% of total inclusions) whereas a few inclusions, in addition to water and CO_2, have quartz. Fluid, transporting gold (silver) mineralization may induced by intrusion of adamellite and syenite dated Yanshanian period, and has reached Daleishan dome, consisted mainly by Dabie metamorphic rocks through Hong'an formation. Sizes of inclusion from mined out veins (vein No I and II) are smaller than those from a mined vein (Vein No X), confirming an ultimate relationship between gold mineralization mobilization, transport and deposition, and inclusion sizes.

In Daleishan goldfield, according to inclusion composition, vapor and liquid may be main agent transport for gold silver in epithermal systems like at concentration (Bajo de la Alumbrera (Argentina) and Grasberg (Indonesia) porphyry copper-gold deposits (Ulrich et al. 1999) where parts-per-million levels of gold have been discovered in vapor.

ACKNOWLEGMENTS

This work would not have been possible without the logistical support of Geological Bureau in charge of Ordos Basin Northeast, Hubei province, China, and we would like to thank Xu Zhiqian, Du Dengwen, both from this bureau, for providing data for some of our figures and reports and for guiding as during field trip. Raman spectroscopy analyses and microscopic observations under Linkam THM-SG 600 of inclusions were conducted at the facilities of Prof. He Mochun at China University of Geosciences, Wuhan, China to whom we express our gratitude.

REFERENCES

[1] Anthony, E., Williams, J., Robert, J. Bowell and Artashes, A. M.， 2009. Gold in Solution. Elements, 5, 281–287. Doi: 10.2113/gselements.5.5.281

[2] Audétat, A., D., Günther, Christoph, A. H., 1998. Formation of a Magmatic-Hydrothermal Ore Deposit: Insights with LA-ICP-MS Analysis of Fluid Inclusions. Science, 279, 5359, 2091-2094.Doi: 10.1126/science.279.5359.2091

[3] Shao Jielian, 1988. Prospecting Mineralogy of Gold Deposit. China University of Geosciences Press, 1988: pp : 38-45 (in Chinese). ISBN 7-5625-1564-6

[4] Ernst, A.J. Burke, 2001. Raman microspectrometry of fluid inclusions. Lithos, 55, 139–158. Doi: 10.1016/S0024-4937 (00)00043-8

[5] Hedenquist, J.W., Reyes, A.G., Simmons, S.F., Taguchi, S., 1992.The thermal and geochemical structure of geothermal and epithermal systems: a framework for interpreting fluid inclusion data. Eur. J. Mineral. 4, 989–1015. ISSN 0935-1221.

[6] Hein, K.A.A., K., Zaw , T., P. Mernagh, 2006. Linking mineral and fluid inclusion paragenetic studies: The Batman deposit, Mt. Todd (Yimuyn Manjerr) goldfield, Australia, Ore Geol. Reviews, 28, 180–200. Doi: 016/j.oregeorev.2005.05.001 www.elsevier.com/locate/oregeorev

[7] Heinrich, C.A., Ryan, C.G., Mernagh, T.P., Eadington, P.J., 1992. Segregation of ore metals between magmatic brine and vapor: a fluid inclusion study using PIXE microanalysis. Econ. Geol., 87, 1566–1583. Doi:10.2113/gsecongeo.87.6.1566 [8] [8] Junji, Yamamoto, H. Kagi, 2003. Micro-Raman densimeter for CO_2 inclusions in mantle-originated fluid inclusions. Chem. Let. 35, 1333-1339

[9] J. Yamamoto, Hiroyuki Kagi, Yoko Kawakami, Naoto Hirano, Masaki Nakamura, 2007. Paleo-Moho depth determined from the pressure of CO_2 fluid inclusions: Raman spectroscopic barometry of mantle- and crust-derived rocks. Earth and Plan. Sc. Lett., 253, 369–377. Doi: 10.1016/j.epsl.2006.10.038

[10] J. Yamamoto, H. Kagi, 2003. Extended micro-Raman densimeter for CO2 inclusions in mantle-originated fluid inclusions. Chem., Lett., 35, 1333-1339.

[11] Lattanzi, P., Curti, E., Bastogi, M., 1989. Fluid inclusion studies on the gold deposits of the Upper Valle Anzasca, northwestern Alps, Italy. Econ. Geol., 84, 1382–1397. Doi: 10.2113/gsecongeo.84.5.1382

[12] Lattanzi, P., 1991. Applications of fluid inclusions in the study and exploration of mineral deposits. Eur. J. Mineral., 3, 689–701. ISSN 0935-1221

[13] Liu, J., Zheng, Zheng, M., Liu, J. and Su, W., 2000. Geochemistry of the La' erma and Qiongmo Au-Se deposits in the western Qinling Mountains, China. Ore Geol. Rev., 17, 1, 91-111. Doi : doi:10.1016/S0169-1368(00)00008-1

[14] Nakamoto, K., 1997. Infrared and Raman spectra of inorganic and coordination compounds. Part A : theory and applications in inorganic chemistry, pp: 401-408. Wiley-Interscience, New York ISBN：9780471743392

[15] Pasteris, J. D., Wopenka, B., Seitz J.C., 1988. Practical Aspects of Quantitative Laser Raman microscope spectroscopy for the study of fluid inclusions Geoch. Cosmochim Acta, 52: 979-988. Doi:10.1016/0016-7037(88)90253-0

[16] Roedder, E., 1984. Fluid inclusions, Review in Min. Mineralogical Association of America, 12: 644 http://rimg.geoscienceworld.org/

[17] Roedder E., 1990. Fluid inclusions Analysis-Prologue and Epilogue. Geoch. Cosmochim Acta, 54: 495-507. Doi: 1 0.1016/0016-7037(90)90347-N

[18] Rusk, B.G. and Reed, M.H., 2002. Scanning electron microscope-cathodoluminescence of quartz reveals complex growth histories in veins from the Butte porphyry copper deposit. Montana. Geology, 30,727-730. Doi: 10.1130/0091-7613(2002) 030<0727:SEMCAO> 2.0.CO;2

[19] Shepherd, T.J., Ranbin, A.H., Alderton, D.H.M., 1985. A Practical Guide to Fluid Inclusion Studies. pp: 239. Blackie, Glasgow. ISBN：0412006014 Takahashi, R., Matsueda, H., Okrugin,V.M and Ono,S.,2007. Epithermal gold-silver

mineralization of the Asachinskoe deposit in South Kamchatka. Russia. Resour. Geol.,57(4), 354-373 (in press).

[20] Takahashi, R., Müller, A., Matsueda, H., Okrugin, V.M., Ono, S., Van den Kerkhof, A.M., Kronz A., Thor, H. Hansteen, Andreas Klügel, 2008. Fluid Inclusion thermobarometry as a tracer for Magmatic Processes. Review in Min. Mineralogical Association of America, 69: 648 http://rimg.geoscienceworld.org/

[21] Andreeva, E.D, 2008. Cathodoluminescence and trace element in quartz: clues to metal precipitation mechanisms at the Asachinskoe gold deposit in Kamchatka.in " origin and evolution of natural diversity. Proceedings of the International Symposium The Origin and evolution of the natural diversity , 1-5 October 2007", H. Okada, S.F. Mawatari, N. Suzuki, P. guatam,eds.Sapporo,175-184. http://hdl.handle.net/2115/38463

[22] Wang, L., J. Zhenmin, H., Mouchun, 2002. Raman spectrum Study on Quartz Exsolution in Omphacite of Eclogite and its Tectonic Significance. Journal of China Univ., 14 (2): 119-126. ISSN 1002-0705

[23] Wark, D.A., Hildreth, W., Spear, F. S., Cherniak, D.J., Watson, E.B.,2007. Pre-eruption recharge of the Bishop magma system. Geology, 35, 235-238. Doi: 10.1130/G23316A.1;

[24] Wiebe, R.A., Wark, D.A, Hawkins, D.P., 2007. Insights from quartz cathodoluminescence zoning into crystallization of the Vinalhaven granite, coastal Maine. Mineral. Petrol., 154, 439-453; Doi :10.1007/s00410-007-0202-z

[25] Watt, G.R., Wright, P., Galloway, S., McLearn, C., 1997. Catholuminescence and trace element zoning in quartz phenocrysts and xenocrysts. Geochim. Cosmochim. Acta, 61, 4337-4348. Doi: 10.1016/S0016-7037(97)00248-2

[26] Wilkinson, J.J., Boyce, A.J., Earls, G., Fallick, A.E., 1999. Gold remobilization by low temperature brines: evidence from the Curraghinalt gold deposit, Northern Ireland. Econ. Geol., 94, 289–296. Doi: 10.2113/gsecongeo.94.2.289

[27] Wilkinson, J.J., 2001. Fluid inclusions in hydrothermal ore deposits. Lithos, 55,229–272. Doi: 10.1016/S0024-4937(00)00047-5

[28] William, D. Carlson, Emily A. McDowell, Masaki Enami, Tadao Nishiyama and Takashi Mouri, 2009. Laser Raman microspectrometry of metamorphic quartz: A simple method for comparison of metamorphic pressures—Corrigendum. American Mineralogist, 94, 291–1292. Doi: 10.2138/am.2009.549

[29] Xiaoming S., Y., Zhang, Dexing X., Weidong S., G., et al., 2009. Crust and mantle contributions to gold-forming process at the Daping deposit, Ailaoshan gold belt, Yunnan, China. Ore Geology Reviews 36, 235 – 249. Doi:10.1016/j.oregeorev.2009.05.002

[30] Y., B. Wu, S., Gao et al., 2009. U-Pb age, trace element, and Hf isotope composition of zircon in quartz vein from eclogite in the west Dabie Mountains: constraints on fluid during early exhumation of ultra-high pressure rocks. American Mineralogist, 94, 303-312. Doi: 10.2138/am.2009.3042

3/1/2010